Calculation of Electronic g-Tensors for Transition Metal Complexes Using Hybrid Density Functionals and Atomic Meanfield Spin-Orbit Operators

MARTIN KAUPP,[1] ROMAN REVIAKINE,[2] OLGA L. MALKINA,[2,3] ALEXEI ARBUZNIKOV,[1] BERND SCHIMMELPFENNIG,[4] VLADIMIR G. MALKIN[2]

[1]*Institut für Anorganische Chemie, Universität Würzburg, Am Hubland, D-97074 Würzburg, Germany*

[2]*Institute of Inorganic Chemistry, Slovak Academy of Sciences, Dubravska Cesta 9, SK-84236 Bratislava, Slovakia*

[3]*Computing Center, Slovak Academy of Sciences, Dubravska Cesta 9, SK-84236 Bratislava, Slovakia*

[4]*Royal Institute of Technology, SCFAB, Department of Biotechnology, Laboratory of Theoretical Chemistry, 10691 Stockholm, Sweden*

Received 25 September 2001; Accepted 7 November 2001

Abstract: We report the first implementation of the calculation of electronic g-tensors by density functional methods with hybrid functionals. Spin-orbit coupling is treated by the atomic meanfield approximation. g-Tensors for a set of small main group radicals and for a series of ten 3d and two 4d transition metal complexes have been compared using the local density approximation (VWN functional), the generalized gradient approximation (BP86 functional), as well as B3-type (B3PW91) and BH-type (BHPW91) hybrid functionals. For main group radicals, the effect of exact-exchange mixing is small. In contrast, significant differences between the various functionals arise for transition metal complexes. As has been shown previously, local and in particular gradient-corrected functionals tend to underestimate the "paramagnetic" contributions to the g-tensors in these cases and thereby recover only about 40–50% of the range of experimental g-tensor components. This is improved to ca. 60% by the B3PW91 functional, which also gives slightly reduced standard deviations. The range increases to almost 100% using the half-and-half functional BHPW91. However, the quality of the correlation with experimental data worsens due to a significant overestimate of some intermediate g-tensor values. The worse performance of the BHPW91 functional in these cases is accompanied by spin contamination. Although none of the functionals tested thus appears to be ideal for the treatment of electronic g-tensors in transition metal complexes, the B3PW91 hybrid functional exhibited the overall most satisfactory performance. Apart from the validation of hybrid functionals, some aspects in the treatment of spin-orbit contributions to the g-tensor are discussed.

 J Comput Chem 23: 794–803, 2002

Key words: density functional theory; EPR spectroscopy; g-tensor; hybrid functionals; spin-orbit coupling

Introduction

The electronic g-tensor is one of the most important parameters of electron paramagnetic resonance spectroscopy (EPR). It contains a wealth of information on the electronic and geometrical structure of molecules or solids with unpaired electrons. In the case of transition metal complexes, qualitative or semiquantitative theoretical treatments of electronic g-tensors have already been used during the early days of EPR spectroscopy, and important models have been developed.[1] However, attempts to calculate g-tensors quantitatively, using first-principles quantum chemical methods, have only been made during the past 5–10 years. These develop-

Correspondence to: M. Kaupp, e-mail: kaupp@mail.uni-wuerzburg.de; or V. G. Malkin, e-mail: malkin@savba.sk

Contract/grant sponsor: Deutsche Forschungsgemeinschaft; contract/grant numbers: SPP1051 and 436-SLK-17/5/00

Contract/grant sponsors: Fonds der Chemischen Industrie and Alexander-von-Humboldt Foundation, and Graduiertenkolleg "Moderne Methoden der Magnetischen Resonanz in der Materialforschung" (Universität Stuttgart)

Contract/grant sponsor: Slovak Grant Agency VEGA; contract/grant number: 2/7203/20

Contract/grant sponsor: COST Chemistry Program; contract/grant number: D9/0002/97

ments have been partly motivated by the recent advent of high-field EPR spectroscopy, which in many cases provides significantly superior resolution of g-tensor components compared to the traditional X-band methods (in particular for organic radicals).[2]

The electronic g-tensor is dominated by contributions from spin-orbit coupling (see theory section) and thus is intrinsically a relativistic property, even for light-element compounds. We thus have to deal appropriately with spin-orbit effects. At the same time, the g-tensor usually requires an adequate treatment of electron correlation. The first *ab initio* treatments of electronic g-tensors at the multireference CI level are due to Lushington et al., within a second-order perturbation theory approach based on the Breit–Pauli Hamiltonian.[3] This method has been shown to yield accurate results for small radicals, containing mainly light main group elements. An alternative HF and MCSCF approach using linear response functions has been developed by Vahtras et al.[4]

These methods are presently not applicable to transition metal complexes of chemically relevant sizes. Here the method of choice could be density functional theory (DFT). A two-component DFT approach for g-tensor calculations at the ZORA level has been developed by van Lenthe et al.[5] The advantage of the two-component methods is the full incorporation of spin-orbit coupling already in the zeroth-order wave function. The presently unsolved problem with this method is the exclusive use of restricted Kohn–Sham wave functions. Two-component g-tensor calculations in an unrestricted DFT framework pose special problems, and they are a field of current research in several groups.

A DFT approach with perturbational treatment of SO coupling has been developed by Schreckenbach and Ziegler (SZ).[6] Like the *ab initio* approaches of Lushington et al. and Vahtras et al., the SZ approach incorporates all perturbations relevant at the Breit–Pauli level. We have recently reported a related perturbation theoretical DFT approach.[7] The main difference to the SZ method is the treatment of the two-electron spin-orbit (SO) operators. While SZ follow the traditional lines of DFT by treating the two-electron contributions by an approximate Kohn–Sham potential, we prefer to use explicit approximations to the full set of one- and two-electron SO integrals (see more detailed discussion in the Theory section). Two approximations have been employed,[7] (a) the atomic meanfield SO method, and (b) SO pseudopotentials.

The accurate treatment of the spin-orbit operators provided by our approach offers the possibility to evaluate the performance of the underlying density functional methods. Good agreement with experiment was found[7] for main group systems, in particular for organic radicals (for more recent applications to bioradicals, cf. refs. 8, and 9). Typically, gradient-corrected functionals in an uncoupled DFT (UDFT) framework produce a systematic overestimate of the dominant paramagnetic contributions to the largest g-tensor components by a few percent. This can be corrected for in a straightforward manner. In contrast, in our systematic validation of the approach for a series of 3d transition metal complexes, local and gradient-corrected functionals reproduced only about 60% and about 50%, respectively, of the experimental range of g-tensor components, even when some outliers at the extreme ends of the value spectrum were excluded (when neglecting two-electron SO contributions, the results were fortuitously in much better agreement with experiment[7]). A significant underestimate of the paramagnetic contributions was also found for 4d and 5d complexes. Very similar results have been obtained by Patchkovskii and Ziegler.[10,11] The two-component ZORA approach of van Lenthe et al.[5] has been reported to give larger paramagnetic contributions.[12] However, this is the result of error compensation, partly due to the restricted Kohn–Sham approach used.

This situation suggests an analogy to the field of NMR chemical shift calculations with DFT methods.[13–15] The slight overestimate of paramagnetic contributions by ca. 10% found typically in calculations with gradient-corrected functionals on main group compounds (but also for main group nuclei in transition metal complexes) contrasts with a significant underestimate for several transition metal nuclei. With gradient-corrected functionals, only about 60% of the shift range is recovered for Fe and about 80% for Rh or Ru shifts, with a number of significant outliers.[16–18] Bühl showed that B3-type hybrid functionals, with admixture of ca. 20% Hartree–Fock exchange, improved the performance to almost 100% of the experimental range and removed the most significant outliers[17–19] (similar results pertain to Co shifts[20]). The reasons for this dependence on the functional have not yet been well understood. However, it is clear[21] that the coupling terms in the perturbation treatment, due to the admixture of Hartree–Fock exchange, lead to the enhanced paramagnetic contributions (and in other cases lead to their overestimation[21,22]). Schreckenbach's analysis[23] of the Fe chemical shift of one of the most critical complexes, ferrocene, suggested that the errors with LDA or GGA functionals arise both from the energy denominators and the perturbation matrix elements, involving rather localized excitations. Similar arguments, based on an overestimate of metal–ligand covalency by the usual functionals, have been used to explain the relatively poor performance of the same functionals for the g-tensors of transition metal complexes.[10]

The calculation and interpretation of electronic g-tensors for transition metal systems is of importance in many fields, including catalysis and metalloenzymes. In view of the close relation between g-tensor and NMR chemical shift calculations, it is interesting to evaluate whether hybrid functionals improve the agreement with experiment for electronic g-tensor calculations. To this end, we have implemented the approach of ref. 7 into a new property code that is able to deal with hybrid functionals and also lacks certain other restrictions of the previous implementation. Here we report the first validation study of the use of hybrid functionals for g-tensor calculations, for a set of small main group radicals, as well as for ten 3d and two 4d transition metal complexes.

Theory

Details of our density-functional theory (DFT) method for the calculation of electronic g-tensors have been given in ref. 7. Here we only summarize the salient features and those aspects that differ from the previous implementation. The g-tensor is calculated as correction, $\Delta\mathbf{g}$, to the free electron value,

$$\mathbf{g} = g_e\mathbf{1} + \Delta\mathbf{g}, \tag{1}$$

with $g_e = 2.002319$. Up to the level of second-order perturbation theory, the g-shift $\Delta\mathbf{g}$ consists of the relevant Breit–Pauli terms

$$\Delta\mathbf{g} = \Delta\mathbf{g}_{SO/OZ} + \Delta\mathbf{g}_{RMC} + \Delta\mathbf{g}_{GC}, \quad (2)$$

of which the "paramagnetic" second-order spin-orbit/orbital Zeeman cross term, $\Delta\mathbf{g}_{SO/OZ}$, dominates (except for extremely small Δg-values).[24] Within the uncoupled DFT (UDFT) approach, using local or gradient corrected density functionals, its cartesian components u,v are computed (in atomic units) as[7]

$$\Delta g_{SO/OZ,uv} = \frac{\alpha^2}{2} g_e \left[\sum_k^{occ(\alpha)} \sum_a^{virt(\alpha)} \frac{\langle\psi_k^\alpha|\mathbf{H}_{SO,v}|\psi_a^\alpha\rangle\langle\psi_a^\alpha|\mathbf{l}_{O,u}|\psi_k^\alpha\rangle}{\varepsilon_k^\alpha - \varepsilon_a^\alpha} - \sum_k^{occ(\beta)} \sum_a^{virt(\beta)} \frac{\langle\psi_k^\beta|\mathbf{H}_{SO,v}|\psi_a^\beta\rangle\langle\psi_a^\beta|\mathbf{l}_{O,u}|\psi_k^\beta\rangle}{\varepsilon_k^\beta - \varepsilon_a^\beta} \right] \quad (3)$$

where α is the fine-structure constant, $\mathbf{H}_{SO}$ is explained below, $\mathbf{l}_{O,u}$ is a spatial component of the orbital Zeeman operator, ψ^σ and ε^σ are spin-polarized Kohn–Sham orbitals and orbital energies, respectively.

Coupling terms do not arise in this treatment, as the exchange-correlation potentials of these functionals do not depend on the induced paramagnetic current density.[25] In the case of hybrid density functionals, the admixture of exact Hartree–Fock exchange into the functional leads to coupling terms, and we have to solve coupled-perturbed Kohn–Sham (CPKS) equations. The coupling terms have to be scaled by the fraction of Hartree–Fock exchange included. The relativistic mass correction term $\Delta\mathbf{g}_{RMC}$ and the one-electron part of the gauge correction term $\Delta\mathbf{g}_{GC}$ are also included in our approach.[7]

At the Breit–Pauli level, a cartesian component of the spatial part of the spin-orbit (SO) operator may be written (in atomic units) as

$$\mathbf{H}_{SO,iu} = \frac{\alpha^2}{4} g_e \left(\sum_N \frac{Z_N \mathbf{L}_{iNu}}{\mathbf{r}_{iN}^3} - \sum_{j\neq i} \frac{\mathbf{L}_{ju}^i}{\mathbf{r}_{ij}^3} - 2 \sum_{j\neq i} \frac{\mathbf{L}_{iu}^j}{\mathbf{r}_{ij}^3} \right), \quad (4)$$

where $Z_N e$ is the charge of nucleus N, $\mathbf{L}_{iNu} = -i(\mathrm{r}_{iN} \times \Delta_i)$, and $\mathbf{L}^i_{ju} = -i(\mathrm{r}_{ij} \times \Delta_j)_u$ ($\mathbf{r}_{iN}$ and $\mathbf{r}_{ij}$ are relative electron-nucleus and electron-electron position vectors). The first term in eq. (4) is the one-electron SO operator due to the charge of the nuclei, the second term is the two-electron SO operator (largely due to the screening of nuclear charge around nucleus N by the core electrons), and the third term is the so-called spin-other-orbit (SOO) term. The latter term arises from the relativistic Breit (transverse) interaction between the electrons.[26] The two-electron terms are of opposite sign than the one-electron terms. They hence reduce the overall spin-orbit coupling and thus the g-shifts.

The Kohn–Sham method is an effective one-electron approach, i.e., electron–electron interactions are not treated by explicit two-electron operators but implicitly via the effective Kohn–Sham potential (including exchange-correlation and Coulomb potentials). This has consequences for the treatment of the two-electron contributions in H_{SO}. Within the Kohn–Sham approach, one has principally two alternatives: (a) employ relativistic density functionals. These cover the Breit interaction and thus the SOO terms. To our knowledge, applications of such functionals have up to now been restricted mainly to atomic calculations and to the energetics of small molecules.[27] (b) Use one of the usual nonrelativistic functionals. Then the SOO terms will not be included. This is the approach usually employed in DFT calculations, for example, in the g-tensor approaches by Schreckenbach and Ziegler[6] or by van Lenthe et al..[5]

In our current implementation, a third possibility is pursued: we step outside the usual Kohn–Sham framework and calculate the SO integrals as is done in traditional wave function approaches, using the Kohn–Sham determinant as an approximation to the wave function of the real, fully interacting system.[28] The spin-orbit (SO) operator, H_{SO}, is computed in the atomic meanfield approximation (AMFI),[29,30] but we have previously also used a full treatment of the one- and two-electron SO integrals.[7,31] The AMFI approach is an excellent and efficient approximation to the full Breit–Pauli treatment (AMFI is also available at the Douglas–Kroll level[29,30]). In particular, it explicitly includes the spin-other-orbit (SOO) terms resulting from the Breit interaction. Our previous calculations have indicated the SOO terms to make a sizeable contribution to the overall two-electron $\Delta\mathbf{g}_{SO/OZ}$ terms (see below).[7] An approximation related to AMFI is the use of SO pseudopotentials.[7] Here the inclusion of the SOO terms depends on the atomic adjustment of the SO pseudopotential parameters.

A deeper analysis of the contributing spin-orbit terms in our explicit treatment shows that in addition to the screening Coulomb-type spin-same-orbit term and the spin-other-orbit terms, further terms arise. The latter can be interpreted as exchange-type spin-orbit terms that simply arise due to the antisymmetry of the Kohn–Sham determinant. These terms may be viewed as exact-exchange corrections to the SO integrals. They are also not present in the normal treatment via a nonrelativistic effective Kohn–Sham potential. These terms lead to a further increase of the two-electron SO contributions and thereby to a slight further decrease of the overall SO coupling. Analyses of calculations for light main group radicals like CO^+ or H_2O^+ show that, in addition to a ca. 20–25% contribution from the SOO terms to $\Delta\mathbf{g}_{SO/OZ}$(2-el.),[7] the extra exchange terms account for another ca. 10–12% of the overall two-electron contributions. As the two-electron contributions reduce the overall g-shift components by ca. 37–40% for these light main group radicals, the SOO terms account for a sizeable reduction by ca. 8–9%, and the additional exchange terms for another reduction by ca. 4–5% (relative to the total g-shifts, the corresponding percentage points are ca. 14% and ca. 7%, respectively). These are nonnegligible contributions. In 3d-complexes, the SOO term has been found to contribute only ca. 12% of the two electron SO terms.[7] Our analyses indicate that the exchange term amounts to another 6%. Due to the very large relative importance of the two-electron terms for transition metal systems (ca. 55% for 3d systems like TiF_3[7]), this results nevertheless in very similar overall relative contributions to the total spin-orbit coupling and g-shift components as for the abovementioned radicals.

Patchkovskii and Ziegler[32] recently argued that our approach will lead to more accurate results than the traditional DFT treatment of spin-orbit coupling in cases where the SOO contribution is sizeable, but that the use of the Kohn–Sham wave function in the explicit evaluation of the SO integrals may lead to errors when correlation effects on the shape of the exchange-correlation hole are large. We doubt that the latter case will be common, as the spin-orbit integrals arise mainly from the inner core shells of the

atoms and are thus relatively insensitive to electron correlation.[26] This is, in fact, one of the main justifications of the atomic meanfield approximation[29,30] used here.

Our previous calculations of g-tensors have used the deMon DFT code[33] in conjunction with the deMon-NMR/EPR property package,[34] into which we have implemented the perturbation theoretical treatment of electronic g-tensors.[7] The deMon code does not allow the use of hybrid functionals, and relies on the use of auxiliary basis sets to fit the charge density and the exchange correlation potential (ν_{xc}). Both the auxiliary basis sets and the orbital basis sets are restricted to angular momentum up to $l = 2$, which is a potential source of inaccuracy in the case of the present open-shell transition metal systems. In this work we use the newly implemented property package MAG,[35] which is based on the HERMIT integral code,[36] and has no restrictions with respect to angular momentum of the basis set. We have, furthermore, implemented a coupled-perturbed Kohn–Sham treatment for use with hybrid functionals. MAG is developed as the property package of our new relativistic DFT code ReSpect.[37] For computational convenience, we have decided for the present study to obtain the (nonrelativistic) Kohn–Sham orbitals from the Gaussian98 program[38] (test calculations with ReSpect provide identical results). For this purpose, an interface from Gaussian98 to MAG has been written. Like ReSpect but unlike deMon, Gaussian98 can treat the four-center Coulomb integrals explicitly and also does not involve any fitting of ν_{xc}. Comparisons with our previous calculations[7] should thus help us to evaluate how severe the extra approximations in deMon are.

Computational Details

The validation calculations are carried out (a) for small set of light main group radicals, (b) for a subset of ten 3d complexes and two 4d complexes ($MoOF_4^-$ and $MoOCl_4^-$) studied in our previous validation of the original g-tensor code.[7] The small main group radicals are common test cases for *ab initio* and DFT approaches.[3,6,7] The d^1 systems MOX_4^- (M = Cr, Mo; X = F, Cl) have already been studied by Patchkowski and Ziegler,[10] and by Malkina et al.[7] Most of the 3d complexes have also been included in a validation of DFT methods for the calculation of hyperfine coupling tensors.[39,40] The molecular structures are those employed in refs. 6, 7, 10, and 39. They generally have been optimized at DFT levels.

The g-tensor calculations were carried out in two steps: first the Kohn–Sham orbitals were generated with the Gaussian98 program.[38] These were then used by the MAG[35] property code to carry out the second-order perturbation calculations [eqs. (2) and (3)[7]]. In the case of local and gradient-corrected functionals, the UDFT approach was used. In the case of hybrid functionals, the admixture of Hartree–Fock exchange leads to an iterative CPKS procedure, where the coupling terms are scaled by the fraction of HF exchange in the corresponding functional. To avoid any artifacts from the localization procedure of an IGLO choice of gauge, we have in this study preferred to use a common gauge at (a) the center of mass for the small main group radicals, and (b) the metal nucleus for the transition metal systems. These choices are expected to be reasonable ones for these systems, as has been evaluated by further test calculations (the g-tensor is generally less gauge dependent than, e.g., NMR chemical shifts[3,6]).

The following exchange-correlation functionals were tested: (a) the local density approximation in form of the Vosko–Wilk–Nusair functional (VWN,[41] corresponding to the VWN5 keyword in the Gaussian98 code); (b) the BP86 GGA functional;[42,43] (c) the B3PW91 functional,[43,44] incorporating ca. 20% HF exchange; d) the half-and-half functional BHPW91,[44,45] including as much as 50% HF exchange.

As in our previous study,[7] the IGLO-III basis[46] was used for the main group radicals. A previously discussed[39] 9s7p4d basis set was used for 3d transition metals, together with IGLO-II basis sets for the ligand atoms.[46] To evaluate the influence of f-polarization functions at the metal, we have also carried out some calculations in which the single f-set of Frenking et al.[47] has been added. An 11s9p6d basis for Mo was constructed by partly decontracting the DZVP basis for Mo,[48] and by replacing the most diffuse p-function by two p-functions[49] and the two most diffuse d-functions by a more flexible 21111 set.[49]

Results

Table 1 summarizes computed and experimental g-shift tensors for the set of small main group radicals. The BP86 results are very similar to the data obtained in ref. 7. Slight differences arise due to the fit of Coulomb and exchange-correlation potentials in the earlier implementation, and to the different choice of gauge origin (IGLO gauge in ref. 7, common gauge at the center of mass in this work). As discussed previously,[7] agreement with experiment is excellent at this computational level, except for the Δg_{33} component of H_2O^+, which is significantly underestimated. For this particular value, the local density approximation (VWN functional) provides better agreement with experiment. However, in the other cases, the larger g-shift components at the VWN level deteriorate the performance somewhat compared to the gradient-corrected functional. Turning to the hybrid functionals, the changes relative to the BP86 results are remarkably small, even for the BHPW91 functional. The small differences between the functionals do not appear to be systematic, and the overall correlation with experiment is quite similar for BP86, B3PW91, and BHPW91 functionals (better than for the local functional). However, the local or gradient-corrected functionals are easier to use for larger systems, due to the lack of coupling terms.

We have sought to understand the unusually large differences between VWN and BP86 results for Δg_{33} of H_2O^+, as these may provide clues (a) to the relatively poor performance of the GGA functional in this particular case, and (b) to the effects expected for transition metal complexes (see below). This g-shift component is dominated by coupling between the β-component of the in-plane HOMO with the (unoccupied) β-component of the out-of-plane SOMO (Table 2). This contribution increases by more than 50% in going from the BP86 to the VWN functional, whereas the corresponding differences for other cases in Table 1 are at most 10–20%. The energies of the frontier orbitals in H_2O^+ appear to be very strongly influenced by spin polarization, and therefore, the energy difference between their β-spin-orbitals is unusually dependent on the functional (Table 2). Thus, in going from the local

Table 1. Comparison of Calculated and Experimental g-Shift Components for Light Main Group Radicals (in ppm)[a].

		VWN	BP86	B3PW91	BHPW91	Exp.[b]	
H_2O^+	Δg_{11}	−175	−175	−175	−174	200	gas
	Δg_{22}	4579	3818	3827	3721	4800	phase
	Δg_{33}	16479	10979	11676	11983	18800	
CO^+	$\Delta g_{\parallel}$	−99	−102	−96	−88	—	gas
	$\Delta g_{\perp}$	−2468	−2356	−2426	−2512	−2400	phase
HCO	Δg_{11}	−165	−164	−176	−184	0	matrix
	Δg_{22}	2376	2264	2303	2320	1500	
	Δg_{33}	−9251	−7723	−7778	−7659	−7500	
C_3H_5	Δg_{11}	−38	−45	−43	−39	0	matrix
	Δg_{22}	585	498	478	443	400	
	Δg_{33}	714	635	615	574	800	
NO_2	Δg_{11}	−593	−586	−628	−725	−300	gas
	Δg_{22}	3591	3555	3888	4286	3900	phase
	Δg_{33}	−12359	−11372	−11918	−12328	−11300	
NF_2	Δg_{11}	−568	−544	−644	−758	−100	matrix
	Δg_{22}	4376	4121	3955	3564	2800	
	Δg_{33}	7175	6537	6547	6258	6200	
MgF	$\Delta g_{\parallel}$	14	14	16	17	−300	matrix
	$\Delta g_{\perp}$	−1919	−1850	−1740	−1573	−1300	

[a]IGLO-III basis set for all atoms.
[b]Cf. refs. 3 and 6 for detailed references to experimental data.

VWN to the gradient-corrected BP86 functional, the energy difference increases from 0.071 a.u. to 0.104 a.u.. This is mainly due to changes in the energy of the unoccupied β-component of the SOMO (the energies of the α-spin-orbitals are also given in Table 2 for comparison). The $\Delta g_{SO/OZ}$ contributions from the HOMO/SOMO coupling are reduced correspondingly, leading to the smaller Δg_{33} component. The orbital energy difference increases even much more for the hybrid functionals. However, there it is compensated for by the coupling terms introduced by HF exchange. Related changes for the other main group radicals are considerably less pronounced. This may explain the unusual sensitivity of this particular g-shift component in H_2O^+ to the functional.

Let us now turn to the transition metal complexes. Table 3 summarizes the g-shift tensors obtained for the full set of complexes and functionals. More details on the selection of experimental data can be found in refs. 7 and 10. Figure 1a–d displays the correlation between theory and experiment for the 3d-complexes, using the VWN, BP86, B3PW91, and BHPW91 functionals, respectively. The dotted line of slope 1.0 indicates ideal agreement, whereas the solid line is the result of a linear regression analysis, including the data for all 3d-complexes. In our previous work,[7] we have not included the most extreme outliers ($\Delta_{\perp}$ of TiF_3, Δg_{zz} of $Cu(NO_3)_2$, and $Cu(acac)_2$) in the regression analysis. Then the local density approximation led to a slope of the regression line of ca. 0.6, indicating that the calculations only reproduced

Table 2. Energies of Frontier Kohn–Sham MOs (in a.u.) and HOMO Contribution to Δg_{33} (in ppm) in H_2O^+ from Different Functionals[a].

		ε_{HOMO}[b]	ε_{SOMO}[c]	$\Delta\varepsilon(\beta)$	Δg_{33} (HOMO)	Δg_{33} (Total)
VWN	α	−0.800	−0.794		16,371	16,479
	β	−0.761	−0.690	0.071		
BP86	α	−0.805	−0.793		10,870	10,979
	β	−0.768	−0.664	0.104		
B3PW91	α	−0.874	−0.856		11,592	11,676
	β	−0.825	−0.599	0.226		
BHPW91	α	−0.975	−0.947		11,931	11,983
	β	−0.912	−0.499	0.413		

[a]The β-components are important for the Δg_{33} component, α-spin-orbitals are given for comparison.
[b]Mainly in-plane lone-pair on oxygen.
[c]Mainly out-of-plane orbital on oxygen.

Table 3. Comparison of Calculated and Experimental g-Shift Components for Transition Metal Complexes (in ppt)[a].

		VWN	BP86	B3PW91	BHPW91	Exp.[b]
$Co(CO)_4$	$\Delta g_{\parallel}$	2.7	3.1	5.9	29.9	3.6
	$\Delta g_{\perp}$	78.0	66.3	88.8	115.9	127.6
$CrOF_4^-$	$\Delta g_{\parallel}$	−21.0	−17.1	−22.7	−33.4	−43
	$\Delta g_{\perp}$	−31.8	−25.8	−30.2	−45.7	−34
$CrOCl_4^-$	$\Delta g_{\parallel}$	19.6	18.2	15.8	6.5	−10
	$\Delta g_{\perp}$	−22.4	−19.3	−25.8	−47.2	−25
$Cu(acac)_2$	Δg_{zz}	107.6	109.4	159.0	299.9	285.2
	Δg_{yy}	26.5	28.0	41.5	75.9	48.7
	Δg_{xx}	30.8	31.8	45.8	79.6	48.7
$Cu(NO_3)_2$	Δg_{zz}	108.7	105.7	157	275	263.8
	Δg_{yy}	24.8	25.2	39.7	71.5	49.9
	Δg_{xx}	27.4	27.3	40.8	71.5	49.9
$Fe(CO)_5^+$	$\Delta g_{\parallel}$	−1.1	−1.4	−3.2	−7.5	−1.5
	$\Delta g_{\perp}$	59.9	50.2	65.9	89.5	79.15
$Mn(CO)_5$	$\Delta g_{\parallel}$	−1.1	−1.3	−2.6	−5.5	−2.3
	$\Delta g_{\perp}$	26.0	22.7	27.4	32.5	35.7
MnO_3	$\Delta g_{\parallel}$	0.5	−0.9	2.9	16.5	−0.4
	$\Delta g_{\perp}$	4.2	4.0	2.7	90.6	4.7
$MoOF_4^-$	$\Delta g_{\perp}$	−45.4	−42.7	−48.3	−60.0	−107
	$\Delta g_{\parallel}$	−46.9	−41.9	−43.3	−47.7	−76
$MoOCl_4^-$	$\Delta g_{\parallel}$	14.0	11.7	7.7	−3.7	−33
	$\Delta g_{\perp}$	−33.7	−31.6	−34.2	−39.7	−55
$Ni(CO)_3H$	$\Delta g_{\parallel}$	1.7	2.7	3.5	13.6	1.9
	$\Delta g_{\perp}$	41.1	45.2	64.1	157.4	65.1
TiF_3	$\Delta g_{\parallel}$	−1.2	−1.3	−1.4	−1.4	−8.6
	$\Delta g_{\perp}$	−50.9	−36.0	−48.8	−71.4	−116

[a]IGLO-II basis for ligands, 9s7p4d basis for 3d metals, 11s9p6d basis for molybdenum.
[b]Cf. refs. 7 and 10 for detailed references to experimental data.

about 60% of the experimental range of g-shift tensor components. In most cases, the present results with the VWN functional (Table 3, Fig. 1a) give very similar results as the previous calculations, with a few notable exceptions: the magnitudes of the (negative) $\Delta_{\perp}$ components in TiF_3 and in $CrOF_4^-$ are notably larger (the previous results were −28.3 ppt and −13.6 ppt, respectively), and the $\Delta_{\perp}$ components in $Fe(CO)_5^+$, $Mn(CO)_5$, and $Cu(NO_3)_2$ have also increased somewhat. Test calculations clearly show that these differences are mostly caused by deficiencies in the previous calculations, due to the use of insufficiently large auxiliary basis sets. Modest differences pertain also to the molybdenum complexes, where ref. 7 gave results obtained with pseudopotentials and SO pseudopotential operators. In all other cases, differences between the previous and present results are at most a few ppt.

Table 4 gives the results of the linear regression analyses for the comparison theory vs. experiment (we do not include the Mo complexes here, as somewhat different performance is expected for 4d systems[7,10,11]). If we exclude again the most extreme outliers, the slope for the VWN data is ca. 0.56, similar to the previous study. Including the complete set of 3d complexes leads to a smaller slope of only ca. 0.44. This indicates again a significant underestimate of the paramagnetic contributions ($\Delta\mathbf{g}_{SO/OZ}$ term) to the g-tensor. We will in the following concentrate on the regression parameters obtained with the complete data set.

Using the gradient-corrected BP86 functional leads to a slightly better correlation coefficient (Table 4; Fig. 1b) but reduces the slope even somewhat further. The reduced paramagnetic contributions agree with previous results (cf. also Table 1), and also with experience for NMR chemical shift calculations.[13–15] If we now include Hartree–Fock exchange, via the B3PW91 functional, we see a significantly increased slope, and also an improved correlation coefficient (Fig. 1c, Table 4). Thus, as expected from the experience with NMR chemical shifts of Fe or Co nuclei, the admixture of Hartree–Fock exchange increases the paramagnetic ($\Delta\mathbf{g}_{SO/OZ}$) contributions, due to the resulting coupling terms. Moreover, the performance for the most extreme outliers at the largest negative and positive Δg values is improved (Table 3). However, in contrast to the NMR chemical shift case, the slope of the regression line is still significantly below 1, i.e., we still underestimate the g-shift range.

Finally, with the BHPW91 "half-and-half" functional, the slope of the regression line has increased to almost 1.0, i.e., we are now covering the correct g-shift range (Table 4, Fig. 1d). This is mainly due to the fact that the magnitude of some of the most extreme g-shift values are now closer to experiment (e.g., $\Delta_{\perp}$ in TiF_3 and Δg_{zz} in the two copper complexes). Unfortunately, the correlation coefficient has deteriorated significantly, and the standard deviation has increased. This is caused by a significant overestimate of

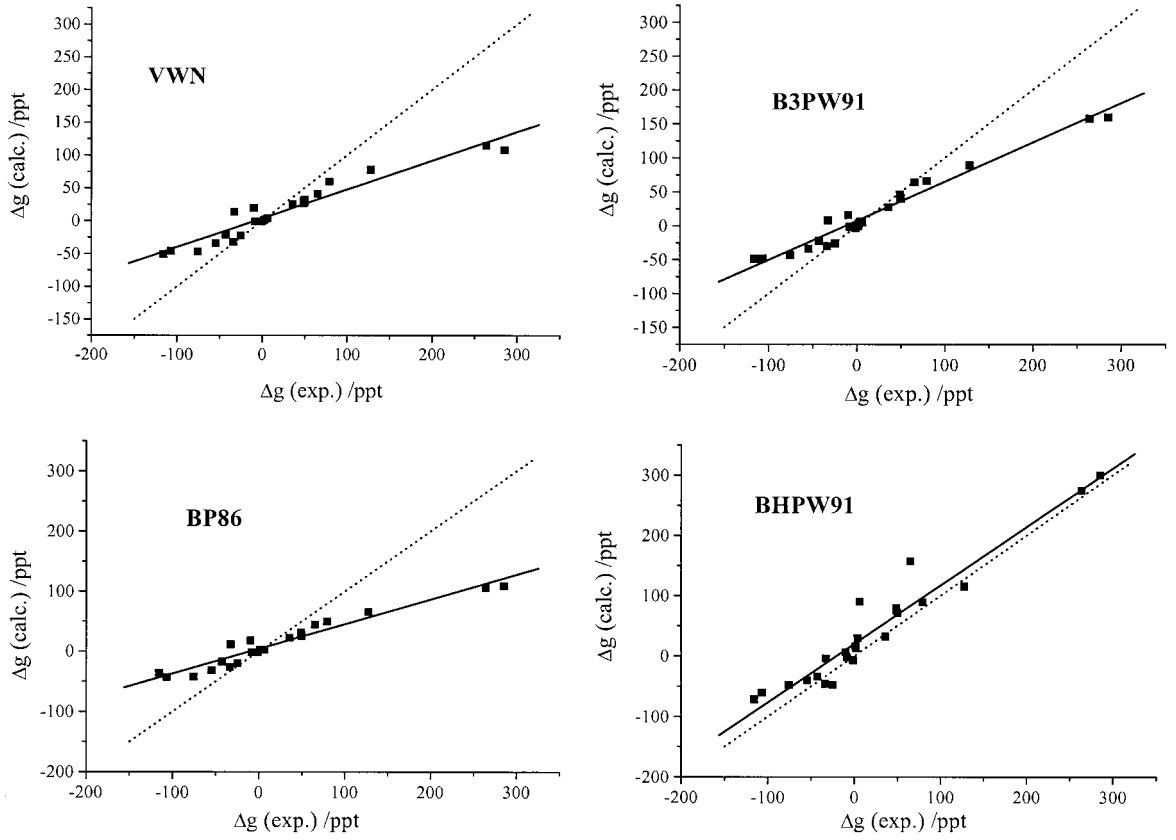

Figure 1. g-Tensor results for 3d complexes with different functionals compared to experiment (data from Table 3, excluding the Mo complexes). The solid line gives the result of linear regression, the dotted line the ideal agreement (slope = 1.0). (a) VWN; (b) BP86; (c) B3PW91; (d) BHPW91.

certain intermediate range values, in particular, both components for MnO_3 and $Ni(CO)_3H$, the $\Delta g_{\|}$ component for $Co(CO)_4$, and the perpendicular components for $Cu(NO_3)_2$ and $Cu(acac)_2$.

In the case of the d^1 complexes MOX_4^-, exact-exchange admixture lowers the $\Delta g_{\|}$ components significantly, whereas the $\Delta g_{\perp}$ components are increased (Table 3). For $CrOCl_4^-$, the wrong sign of $\Delta g_{\|}$ compared to experiment remains even at the BHPW91 level (while $\Delta g_{\perp}$ becomes too negative). The wrong order of the two components remains for $CrOF_4^-$. For all four systems, the negative charge of the complex may lead to significant environmental effects, which have not been covered in the present calculations. This may explain part of the discrepancies with experiment.

Table 5 shows the effect of adding an f-polarization function to the metal (B3PW91 results). In most cases, the influence of the f-functions is very small. In those cases where the change exceeds a few ppt (e.g., Δg_{zz} in $Cu(NO_3)_2$, $\Delta g_{\perp}$ in $Ni(CO)_3H$), it corresponds to an increase of the g-shift. The agreement with experiment is not affected noticeably by the inclusion or omission of one metal f-function.

Table 4. Results of Linear Regression Analyses for Comparisons between Theory and Experiment for *g*-Shift Tensors of 3d Complexes.[a]

	VWN	BP86	B3PW91	BHPW91
Intercept B (ppt)[a]	3.7	4.8	6.6	17.9
Slope A[a]	0.438	0.403	0.580	0.992
Regression coefficient	0.963	0.972	0.981	0.956
Standard deviation SD (ppt)	11.5	9.1	10.7	28.5

[a] $\Delta g_{ii}(\text{calc.}) = A\ \Delta g_{ii}(\text{exp.}) + B$. SD $= \sqrt{\frac{1}{n-1}\sum_{j=1}^{n}(g_{ii,j} - \bar{g}_{ii})^2}$. Cf. results in Table 3.

Discussion

The admixture of Hartree–Fock exchange, and the inclusion of the corresponding coupling terms in the perturbation treatment, does not affect the g-tensor results for light main group radicals much. However, it has a significant effect on the g-tensors of transition metal systems. In the latter case, the $\Delta\mathbf{g}_{SO/OZ}$ contributions to the g-tensors are increased, and the agreement with experiment is improved regarding the overall range covered. These results are consistent with experience for NMR chemical shift calculations on 3d (Fe, Co) or 4d (Rh) transition metal nuclei.[13,17,19] In contrast to the latter case, the B3PW91 functional (which includes ca. 20% of

Table 5. Effect of *f*-Polarization Functions on *g*-Shift Components (in ppt).[a]

		Without *f*-function	With *f*-function
$Co(CO)_4$	$\Delta g_{\parallel}$	5.9	9.7
	$\Delta g_{\perp}$	88.8	87.4
$CrOF_4^-$	$\Delta g_{\parallel}$	−22.7	−22.3
	$\Delta g_{\perp}$	−30.2	−28.9
$CrOCl_4^-$	$\Delta g_{\parallel}$	15.8	14.9
	$\Delta g_{\perp}$	−25.8	−25.8
$Cu(acac)_2$	Δg_{zz}	159.0	173.6
	Δg_{yy}	41.5	45.7
	Δg_{xx}	45.8	49.7
$Cu(NO_3)_2$	Δg_{zz}	157.0	163.1
	Δg_{yy}	39.7	40.6
	Δg_{xx}	40.8	41.7
$Fe(CO)_5^+$	$\Delta g_{\parallel}$	−3.2	−3.2
	$\Delta g_{\perp}$	65.9	65.9
$Mn(CO)_5$	$\Delta g_{\parallel}$	−2.6	−2.6
	$\Delta g_{\perp}$	27.4	27.2
MnO_3	$\Delta g_{\parallel}$	2.9	−0.6
	$\Delta g_{\perp}$	2.7	4.4
$MoOF_4^-$	$\Delta g_{\parallel}$	−48.3	−50.5
	$\Delta g_{\perp}$	−43.3	−43.0
$MoOCl_4^-$	$\Delta g_{\parallel}$	7.7	6.0
	$\Delta g_{\perp}$	−34.2	−34.2
$Ni(CO)_3H$	$\Delta g_{\parallel}$	3.5	5.0
	$\Delta g_{\perp}$	64.1	71.9
TiF_3	$\Delta g_{\parallel}$	−1.4	−1.4
	$\Delta g_{\perp}$	−48.8	−48.8

[a]B3PW91 results.

Hartree–Fock exchange) nevertheless still underestimates the range of g-tensor values covered significantly. However, of the functionals studied here, it provides the overall best performance when both slope *and* correlation coefficient of the linear regression analysis are considered.

A further increase of the slope, almost to the ideal value, is obtained by increasing the fraction of HF exchange to 50%, in the BHPW91 functional. However, there is a price to pay. The correlation coefficient deteriorates, due to a significant overestimate of a number of intermediate g-shift components. The reasons for the less systematic agreement with experiment become clearer when we look at the S^2 expectation values in Table 6. Although these values pertain to the noninteracting reference system of Kohn–Sham theory, they nevertheless provide useful clues on the quality of the overall calculation.[50] In our recent studies of hyperfine couplings for 3d transition metal complexes,[39] we noted that admixture of HF exchange into the functional may in some cases lead to significant spin contamination (i.e., the S^2 values become significantly larger than, for example, the nominal 0.75 for a pure doublet state), and thereby to a significant deterioration of dipolar hyperfine couplings (and also to increased errors for the isotropic hyperfine coupling constants). In other cases no problems with spin contamination arose. Detailed analyses showed that,[40] as a rule of thumb, spin contamination is a problem particularly in those cases where the singly occupied molecular orbitals (SOMO) have significant metal–ligand antibonding character (either for σ- or for strong π-interactions), roughly speaking when they point towards the ligands and not in between them. In this case, certain doubly occupied valence orbitals (mainly those corresponding to the bonding combination) experience significant spin polarization in an unrestricted Kohn–Sham treatment. Admixture of Hartree–Fock exchange enhances this valence-shell spin polarization, and therefore, may lead to significant spin contamination and a serious deterioration of the overall quality of the wave function.[40]

Indeed, the largest S^2 expectation values are found with the BHPW91 functional (Table 6), in particular, for complexes like MnO_3 (this is the most extreme case), $Co(CO)_4$, or $Ni(CO)_3H$. These are also the cases where the BHPW91 results overshoot most significantly some specific Δg components (Table 3). Some of the small main group radicals (cf. CO^+ or C_3H_5 in Table 6) also exhibit an S^2 value of the Kohn–Sham wavefunction significantly larger than 0.75 with the BHPW91 functional. In these cases no particularly large effects on the g-tensors could be noted.

Conclusions

We have implemented the use of hybrid functionals in calculations of electronic g-tensors. The use of an accurate atomic meanfield approximation to the full molecular spin-orbit operator has allowed the validation of the accuracy of different DFT approaches in calculating g-tensors for both main group radicals and transition metal complexes.

For light main group radicals, g-tensors computed with hybrid functionals do not differ much from those obtained previously with gradient-corrected functionals. The extra computational effort involved (solution of Coupled-Perturbed Kohn–Sham equations) may thus not be justified. The unusually large sensitivity of the

Table 6. S^2 Expectation Values of the Kohn–Sham Determinant.

	VWN	BP86	B3PW91	BHPW91
$Co(CO)_4$	0.761	0.761	0.765	0.815
$CrOF_4^-$	0.761	0.761	0.771	0.798
$CrOCl_4^-$	0.765	0.768	0.784	0.836
$Cu(NO_3)_2$	0.751	0.751	0.753	0.755
$Cu(acac)_2$	0.750	0.752	0.753	0.754
$Fe(CO)_5^+$	0.758	0.757	0.763	0.765
$Mn(CO)_5$	0.753	0.753	0.758	0.763
MnO_3	0.769	0.785	0.887	1.833
$MoOF_4^-$	0.753	0.753	0.755	0.759
$MoOCl_4^-$	0.753	0.754	0.757	0.762
$Ni(CO)_3H$	0.752	0.753	0.755	0.788
TiF_3	0.753	0.753	0.753	0.753
H_2O^+	0.752	0.752	0.753	0.754
CO^+	0.762	0.763	0.771	0.788
HCO	0.751	0.752	0.754	0.757
C_3H_5	0.757	0.766	0.783	0.826
NO_2	0.751	0.752	0.754	0.759
NF_2	0.752	0.752	0.754	0.757
MgF	0.750	0.750	0.750	0.750

[a]Basis sets as in Tables 1 and 3.

Δg_{33} component of H_2O^+ to the choice of (gradient-corrected vs. local) density functional has been traced back to large changes in the orbital energy of the unoccupied β-component of the SOMO.

For transition metal complexes, the significant underestimate of the experimental range of g-tensor components by local and (even more so) gradient corrected functionals is partly corrected by employing hybrid functionals. However, while the B3PW91 functional shows good correlation with experiment, it still covers a significantly too small range. Use of the BHPW91 functional, i.e., admixture of 50% Hartree–Fock exchange, leads to a reproduction of the correct range but deteriorates the overall correlation. This is due to significant spin contamination in cases where the SOMO has appreciable metal–ligand antibonding character. Exact-exchange admixture has a much more pronounced effect on the g-tensors of transition metal complexes (or on the NMR chemical shifts of transition metal nuclei[13,17–20]) than for simpler main group systems. This may be related to the presence of particularly low-lying excited states (of mainly local metal character). We cannot presently exclude that a current dependency of the exchange-correlation functionals (which is presently neglected in local or GGA functionals but partly included by exact-exchange admixture) may have a larger influence in the case of transition metals. Generally, further studies will be needed, including a larger set of 4d and 5d complexes, to judge the overall accuracy of hybrid DFT approaches in g-tensor calculations on transition metal systems.

Acknowledgments

We are grateful to Drs. Ch. van Wüllen (Berlin) and E. Engel (Frankfurt) for helpful discussions on spin-orbit operators.

References

1. Abragam, A; Bleaney, B. Electron Paramagnetic Resonance of Transition Ions; Claredon Press: Oxford, 1970; Symons, M. C. R. Chemical and Biochemical Aspects of Electron-Spin Resonance Spectroscopy; Van Nostrand: New York, 1978; Atherton, N. M. Principles of Electron Spin Resonance; Prentice Hall: New York, 1993.
2. See, e.g., Möbius, K. In Biological Magnetic Resonance; Berliner, L. J.; Reuben, J, Eds.; Plenum Press: New York, 1993, p. 253, vol. 13; Prisner, T. F. In Advances in Magnetic and Optical Resonance; Warren, W., Ed.; Academic Press: New York, 1997, p. 245, vol. 20.
3. (a) Lushington, G. H.; Grein, F. Theor Chim Acta 1996, 93, 259; (b) Bruna, P.; Lushington, G. H.; Grein, F. Chem Phys 1997, 225, 1; (c) Lushington, G. H. PhD thesis, The University of New Brunswick, Canada, 1996.
4. Engström, M.; Minaev, B.; Vahtras, O.; Ågren, H. Chem Phys 1998, 237, 149; Vahtras, O.; Minaev, B.; Ågren, H. Chem Phys Lett 1997, 281, 186.
5. van Lenthe, E.; Wormer, P. E. S.; van der Avoird, A. J Chem Phys 1997, 107, 2488.
6. Schreckenbach, G.; Ziegler, T. J Phys Chem A 1997 101, 3388.
7. Malkina, O. L.; Vaara, J.; Schimmelpfennig, B.; Malkin, V. G.; Kaupp, M. J Am Chem Soc 2000, 122, 9206.
8. Kaupp, M.; Remenyi, C.; Vaara, J.; Malkina, O. L.; Malkin, V. G. J Am Chem Soc, in press.
9. Engström, M. PhD thesis, University of Linköping, Sweden, 2001.
10. Patchkovskii, S.; Ziegler, T. J Chem Phys 1999, 111, 5730.
11. Patchkovskii, S.; Ziegler, T. J Am Chem Soc 2000, 122, 3506.
12. van Lenthe, E.; van der Avoird, A.; Hagen, W. R.; Reijerse, E. J. J Phys Chem A 2000, 104, 2070; Stein, M.; van Lenthe, E.; Baerends, E. J.; Lubitz, W.; J Phys Chem A, 2001, 105, 416; Stein, M.; van Lenthe, E.; Baerends, E. J.; Lubitz, W. J Am Chem Soc 2001, 123, 5839; See also: Carl, P. J.; Isley, S. L.; Larsen, S. C. J Phys Chem A 2001, 105, 4563.
13. Bühl, M.; Kaupp, M.; Malkin, V. G.; Malkina, O. L. J Comp Chem 1999, 20, 91.
14. Schreckenbach, G.; Ziegler, T.; Theor Chem Acc 1998, 2, 71.
15. Kaupp, M.; Malkin, V. G.; Malkina, O. L. In Encyclopedia of Computational Chemistry; Schleyer, P. v. R., Ed.; Wiley: New York, 1998.
16. Bühl, M.; Malkina, O. L.; Malkion, V. G. Helv Chim Acta 1996, 79, 742.
17. Bühl, M. Organometallics 1997, 16, 261.
18. Bühl, M.; Gaemers, S.; Elsevier, C. J. Chem Eur J 2000, 6, 3272.
19. Bühl, M. Chem Phys Lett 1977, 267, 251.
20. (a) Godbout, N.; Havlin, R.; Salzmann, R.; Debrunner, P. G.; Oldfield, E. J Phys Chem A 1998, 102, 2342; (b) Mahon, M. C.; deDios, A. C.; Godbout, N.; Salzmann, R.; Laws, D. D.; Le, H.; Havlin, R. H.; Oldfield, E. J Am Chem Soc 1998, 120, 4784; Godbout, N.; Oldfield, E. J Am Chem Soc 1997, 119, 8065.
21. Kaupp, M.; Malkina, O. L.; Malkin, V. G. J Chem Phys 1997, 106, 9201.
22. Bühl, M. Chem Eur J 1999, 5, 3514.
23. Schreckenbach, G. J Chem Phys 1999, 110, 11936.
24. See, e.g.: Harriman, J. E. Theoretical Foundations of Electron Spin Resonance; Academic Press: New York, 1978.
25. For a discussion of current-density functional theory in the context of magnetic resonance parameters, see: van Wüllen, Ch. J Chem Phys 1995, 102, 2806, and references therein.
26. Hess, B. A.; Marian, C. M. In Computational Molecular Spectroscopy; Jensen, P.; Bunker, P. R., Eds.; Wiley: Sussex, 2000, p. 237.
27. For relativistic exchange-correlation functionals, c.f., e.g., Engel, E.; Facco Bonetti, A.; Keller, S.; Andrejkovics, I.; Dreizler, R. M. Phys Rev A 1998, 58, 964; Engel, E.; Keller, S.; Dreizler, R. M. Phys Rev A 1996, 53, 1367; Mayer, M.; Häberlen, O. D.; Rösch, N. Phys Rev A 1996, 54, 4775.
28. For a general, lucid discussion of the role of the Kohn–sham wave function, see, e.g., Baerends, E. J.; Gritsenko, O. V. J Phys Chem A 1997, 101, 5283.
29. Hess, B. A.; Marian, C.; Wahlgren, U.; Gropen, O. Chem Phys Lett 1996, 251, 365.
30. The AMFI code used is due to: Schimmelpfennig, B. Atomic Spin-Orbit Meanfield Integral Program; Stockholms Unviersitet, Sweden, 1996.
31. Malkina, O. L.; Schimmelpfennig, B.; Kaupp, M.; Hess, B. A.; Chandra, P. Wahlgren, U.; Malkin, V. G. Chem Phys Lett 1998, 296, 93.
32. van Wüllen, Ch., personal communication.
33. deMon program: Salahub, D. R.; Fournier, R.; Mlynarski, P.; Papai, I.; St-Amant, A.; Ushio, J. In Labanowski, J.; Andzelm, J., Eds.; Density Functional Methods in Chemistry; Springer: New York, 1991; St-Amant, A.; Salahub, D. R. Chem Phys Lett 1990, 169, 387.
34. Malkin, V. G.; Malkina, O. L.; Eriksson, L. A.; Salahub, D. R. In Modern Density Functional Theory: A Tool for Chemistry; Theoretical and Computational Chemistry; Seminario, J. M.; Politzer, P., Eds.; Elsevier: Amsterdam, 1995, p. 273, vol. 2.
35. Malkin, V. G.; Malkina, O. L.; Reviakine, R.; Schimmelpfennig, B.; Kaupp, M. MAG, version 1.0.
36. HERMIT is the integral package of Dalton, a molecular electronic structure program, Release 1.2 (2001), written by Helgaker, T; Jensen, H. J. Aa.; Jørgensen, P.; Olsen, J.; Ruud, K.; Ågren, H.; Auer, A. A.;

Bak, K. L.; Bakken, V.; Christiansen, O.; Coriani, S.; Dahle, P.; Dalskov, E. K.; Enevoldsen, T.; Fernandez, B.; Hättig, C.; Hald, K.; Halkier, A.; Heiberg, H.; Hettema, H.; Jonsson, D.; Kirpekar, S.; Kobayashi, R.; Koch, H.; Mikkelsen, K. V.; Norman, P.; Packer, M. J.; Pedersen, T. B.; Ruden, T. A.; Sanchez, A.; Saue, T.; Sauer, S. P. A.; Schimmelpfennig, B.; Sylvester–Hvid, K. O.; Taylor, P. R.; Vahtras, O.

37. Malkin, V. G.; Malkina, O. L.; Reviakine, R.; Schimmelpfennig, B.; Arbuznikov, A.; Kaupp, M. ReSpect, version 1.0.
38. Frisch, M. J.; Trucks, G. W.; Schlegel, H. B.; Scuseria, G. E.; Robb, M. A.; Cheeseman, J. R.; Zakrezewski, V. G.; Montgomery, J. A., Jr.; Stratmann, R. E.; Burant, J. C.; Dapprich, S.; Millam, J. M.; Daniels, A. D.; Kudin, K. N.; Strain, M. C.; Farkas, O.; Tomasi, J.; Barone, V.; Cossi, M.; Cammi, R.; Mennucci, B.; Pomelli, C.; Adamo, C.; Clifford, S.; Ochterski, J.; Petersson, G. A.; Ayala, P. Y.; Cui, Q.; Morokuma, K.; Malick, D. K.; Rabuck, A. D.; Raghavachari, K.; Foresman, J. B.; Cioslowski, J.; Oritz, J. V.; Baboul, A. G.; Stefanov, B. B.; Liu, G.; Liashenko, A.; Piskorz, P.; Komaromi, I.; Gomperts, R.; Martin, R. L.; Fox, D. J.; Keith, T.; Al-Laham, M. A.; Peng, C. Y.; Nanayakkara, A.; Gonzalez, C.; Challacombe, M.; Gill, P. M. W.; Johnson, B.; Chen, W.; Wong, M. W.; Andres, J. L.; Gonzalez, C.; Head–Gordon, M.; Replogle, E. S.; Pople, J. A. Gaussian 98, Revision A.7; Gaussian, Inc.: Pittsburgh, PA, 1998.
39. Munzarová, M.; Kaupp, M. J Phys Chem 1999, 103, 9966.
40. Munzarová, M. L.; Kubáček, P.; Kaupp, M. J Am Chem Soc 2000, 112, 11900.
41. Vosko, S. H.; Wilk, L.; Nusair, M. Can J Chem 1980, 58, 1200.
42. Becke, A. D. Phys Rev A 1988, 38, 3098; Perdew, J. P. Phys Rev B 1986, 33, 8822.
43. Becke, A. D. J Chem Phys 1993, 98, 5648.
44. Perdew, J. P.; Wang, Y. Phys Rev B 1992, 45, 13244; Perdew, J. P. In Electronic Structure of Solids; Ziesche, P.; Eischrig, H., Eds.; Akademie Verlag: Berlin, 1991; Perdew, J. P.; Chevary, J. A.; Vosko, S. H.; Jackson, K. A.; Pederson, M. R.; Singh, D. J.; Fiolhais, C. Phys Rev B 1992, 46, 6671.
45. Becke, A. D. J Chem Phys 1993, 98, 1372.
46. Kutzelnigg, W.; Fleischer, U.; Schindler, M. In NMR—Basic Principles and Progress; Springer: Heidelberg, 1990, p. 165, vol. 23.
47. Ehlers, A. W.; Böhme, M.; Dapprich, S.; Gobbi, A.; Höllwarth, A.; Jonas, V.; Köhler, K. F.; Stegmann, R.; Veldkamp, A.; Frenking, G. Chem Phys Lett 1993, 216, 111.
48. DZVP basis: Godbout, N.; Salahub, D. R.; Andzelm, J.; Wimmer, E. Can J Chem 1992, 70, 560. Parameters for Mo taken from the deMon basis set library.
49. Andrae, D.; Häussermann, U.; Dolg, M.; Stoll, H.; Preuss, H. Theor Chim Acta 1990, 77, 123.
50. See, e.g., Baker, J.; Scheiner, A.; Andzelm, J. Chem Phys Lett 1993, 216, 380.